

Treatment of backscattering in a gas of interacting fermions confined to a one-dimensional harmonic atom trap

Gao Xianlong and W. Wonneberger

*Abteilung für Mathematische Physik,
Universität Ulm, D89069 Ulm, Germany*

(Dated: December 2, 2024)

Abstract

An asymptotically exact many body theory for spin polarized interacting fermions in a one-dimensional harmonic atom trap is developed using the bosonization method and including backward scattering. In contrast to the Luttinger model, backscattering in the trap generates one-particle potentials which must be diagonalized simultaneously with the two-body interactions. Inclusion of backscattering becomes necessary because backscattering is the dominant interaction process between confined identical one-dimensional fermions. The bosonization method is applied to the calculation of one-particle matrix elements at zero temperature. A model for the interaction coefficients is developed along the lines of the Luttinger model with only one coupling constant K . With these results, occupation probabilities of oscillator states, particle densities, Wigner function, and the central pair correlation function are calculated and displayed for large fermion numbers. It is shown how interactions modify these quantities. The anomalous dimension of the pair correlation function in the center of the trap is also discussed and found to be in accord with the Luttinger model.

PACS numbers: PACS numbers: 71.10.Pm, 05.30.Fk, 03.75.Fi

I. INTRODUCTION

The achievement of Bose-Einstein condensation in dilute ultracold gases [1] stimulated the theoretical interest in trapped fermionic many body systems [2, 3, 4], especially their superfluid properties [5, 6, 7, 8]. Recent experimental successes in obtaining degeneracy in three-dimensional Fermi vapors [9, 10, 11, 12, 13] intensified the interest in confined Fermi gases.

Using microtrap technology [14, 15, 16, 17, 18], it is conceivable to realize a neutral ultracold quantum gas of trapped quasi one-dimensional degenerate fermions.

In many cases, identical spin polarized fermions experience only a weak residual interaction because s-wave scattering is forbidden. This makes the question of interactions in a one-component spin polarized fermion system somewhat academic. A possible exception is the electric dipole-dipole interaction in the case of polar molecules [19].

The confinement of a trapped ultracold gas can be realized by a harmonic potential. We have developed an asymptotically exact theory of interacting one-dimensional fermions confined to a harmonic trap. It is based on the bosonization method known from the theory of Luttinger liquids (cf. [20, 21, 22, 23]) and exploits the linearity of the energy spectrum of free oscillator states. The method was presented in [24] for the one-component gas with forward scattering and extended in [25] to the case of two components. This model must be seen as a soft boundary alternative to the well studied case of one-dimensional interacting fermions confined by hard walls [26, 27, 28, 29, 30, 31, 32].

Meanwhile, an investigation of the interaction matrix elements for one-dimensional identical fermions in the harmonic trap revealed [33] that backscattering dominates forward scattering unless the pair potential is long ranged. Unlike in the case of the Luttinger model, backscattering cannot be taken into account by merely renormalizing the forward coupling constants. This is due to the one-branch structure of the present model, which generates one-particle potentials from the backward scattering when the latter is brought into the form of an effective forward scattering. These one-particle potentials must be diagonalized simultaneously with the two particle interactions from forward scattering. We solve this problem by supplementing the squeezing transformation with an appropriate displacement transformation.

The paper is organized as follows: Sec. II describes the model and classifies the scattering

processes for fermions in the one-dimensional harmonic trap. Sec. III gives the solution of the backscattering problem using the bosonization method for the one-particle matrix elements. Sec. IV presents results for several quantities of interest: Occupation probabilities, particle and momentum densities, and the central pair correlation function, which are all derivable from the one-particle matrix elements. We employ a model of the interaction coefficients developed in analogy with the Luttinger model. It is characterized by just one coupling constant K and by a small decay parameter $r \ll 1$. This description is developed in the Appendix.

II. THEORY

A. Description of the model

We consider spin polarized fermionic atoms interacting via the pair interaction operator

$$\hat{V} = \frac{1}{2} \sum_{mnpq} V(m, p; q, n) (\hat{c}_m^\dagger \hat{c}_q) (\hat{c}_p^\dagger \hat{c}_n). \quad (1)$$

The fermions are confined to a highly anisotropic axially symmetric harmonic trap. The trap potential is

$$V(x, y, z) = \frac{1}{2} m_A \omega_\ell^2 z^2 + \frac{1}{2} m_A \omega_\perp^2 (x^2 + y^2) \equiv V_z(z) + V_\rho(\rho). \quad (2)$$

The atom mass is denoted m_A and z is the one-dimensional coordinate in the elongated axial direction of the trap. The trap frequencies are ω_ℓ and $\omega_\perp \gg \omega_\ell$. The quasi one-dimensional Fermi gas is characterized by N ($\leq \omega_\perp/\omega_\ell$) identical fermions filling the first N one-particle levels

$$\hbar\omega_n = \hbar\omega_\ell(n + 1/2), \quad n = 0, 1, \dots \quad (3)$$

of the one-dimensional harmonic potential V_z , while the transverse part of each unperturbed wave function remains the transverse ground state $\psi_{\perp 0}(x)\psi_{\perp 0}(y)$.

The unperturbed one-dimensional Fermi energy is

$$\epsilon_F = \hbar\omega_\ell(N - 1) + \frac{1}{2}\hbar\omega_\ell = \hbar\omega_\ell(N - \frac{1}{2}). \quad (4)$$

The Fermi energy is only slightly smaller than the excitation energy $\hbar\omega_\perp$ of the first excited transverse state in the case of $N = N_{max} =$ largest integer in ω_\perp/ω_ℓ . We have in mind a situation when the filling factor $F \equiv N/N_{max}$ is small enough so that the Fermi level is well below this excitation energy. The above assumption about the transverse wave function is then justified. Furthermore, there still exists a macroscopic number of possible excitations of the one-dimensional Fermi sea that do not violate this condition.

The operators in \hat{c}_m^\dagger and \hat{c}_q in Eq. (1) denote fermion creation and destruction operators, respectively. They obey the fermionic algebra $\hat{c}_m\hat{c}_n^\dagger + \hat{c}_n^\dagger\hat{c}_m = \delta_{m,n}$. This ensures that each oscillator state with single particle wave function

$$\psi_n(z) = \sqrt{\frac{\alpha}{2^n n! \pi^{1/2}}} e^{-\alpha^2 z^2/2} H_n(\alpha z) \quad (5)$$

and energy $\epsilon_n = \hbar\omega_n$ is at most singly occupied.

The intrinsic length scale of the system is the oscillator length $l = \alpha^{-1}$ where α is defined by $\alpha^2 = m_A\omega_\ell/\hbar$. H_n denotes a Hermite polynomial.

B. Classification of coupling coefficients

We are interested in the modification of the zero temperature Fermi sea due to the interaction (1). This problem is different from that of scattering between excitations above the Fermi sea, which, in the present one-dimensional context, are probably not quasi particles.

First of all, we must classify the coupling coefficients in Eq. (1). There are 24 coupling coefficients $V(m, p; q, n)$ for any set of four distinct integers. Due to the symmetries ($m \leftrightarrow q$), ($n \leftrightarrow p$), and ($[m, q] \leftrightarrow [n, p]$) only three coupling coefficients remain.

It is shown in [33] that among them, those with index combinations $n = m + p - q$, $n = p + q - m$, and $n = m + q - p$ dominate, provided the fermion number N is large. It is here, where the fermionic nature of the quantum gas becomes relevant.

We can thus write

$$V(m, p; q, n) \rightarrow V_a \delta_{m-q, n-p} + V_b \delta_{q-m, n-p} + V_c \delta_{m+q, n+p}. \quad (6)$$

Qualitatively, this can be understood as follows: The single particle states ψ_n well inside the trap are superpositions of plane wave states $\exp(ik_n z)$ with $k_n = \pm\alpha\sqrt{2n+1}$. For $N \gg 1$,

the relevant states are near the Fermi energy and thus $|k_n| \approx k_F = \alpha\sqrt{2N-1}$. Here, k_F denotes the Fermi wave number.

According to Eq. (1), incoming states $\{n, q\}$ are transformed into $\{p, m\}$ in the collision process and the momenta of these states are (approximately, because of the weakly inhomogeneous trapping potential) conserved. Denoting a state with $k_n \approx -k_F$ by $(-n)$, three distinct collision processes can be discriminated:

$$\{n, q\} \rightarrow \{p, m\}, \quad \{n, (-q)\} \rightarrow \{p, (-m)\}, \quad \{n, (-q)\} \rightarrow \{(-p), m\}. \quad (7)$$

Processes with strict momentum conservation dominate: This explains the Kronecker symbols in the approximate relation (6). Momentum transfer in the first two cases is small, thus describing forward scattering. In the last case, the momentum transfer is about $2k_F$, which corresponds to backward scattering.

The first two cases were considered in [24, 25]. The last one requires an extension of the bosonization method, which is the aim of the present paper.

The couplings V_a , V_b , and V_c are the analogues of the Luttinger model couplings g_4 , g_2 , and g_1 , respectively [20, 22, 23]. In contrast to the Luttinger case, it was found in [33] that in a gas of identical fermions confined to the harmonic trap, forward scattering is almost completely suppressed so that backscattering is the dominant interaction process, unless the pair interaction potential is of long range.

III. BACKSCATTERING AND BOSONIZATION

The treatment of forward scattering is described in [24, 25]. Though we will include all three types of scattering in the final formulae, we give here only the extensions necessary for the inclusion of the backscattering interaction coefficients

$$V(m, p; q, n) = V_c(|q - p|) \delta_{m+q, n+p}. \quad (8)$$

Substituting these interaction coefficients into Eq. (1) and reordering operators gives

$$\hat{V}_c = -\frac{1}{2} \sum_{mp, v \neq 0} V_c(|v|) (\hat{c}_m^\dagger \hat{c}_{m+v}) (\hat{c}_p^\dagger \hat{c}_{p+v}) + \frac{1}{2} \sum_{m, v \neq 0} V_c(|v|) (\hat{c}_{m+v}^\dagger \hat{c}_{m-v}). \quad (9)$$

We omitted terms which are proportional to the fermion number operator by setting $V_c(0) = 0$. The second term is a one-particle operator, which appears due to the backscattering.

The essential requirement of the bosonization method is the possibility to express all operators entirely in terms of density fluctuation operators. It is still met in the present case: Introducing the density fluctuation operators

$$\hat{\rho}(p) \equiv \sum_q \hat{c}_{q+p}^\dagger \hat{c}_q, \quad (10)$$

or, more conveniently, canonical boson operators related to them by:

$$\hat{\rho}(p) = \begin{cases} \sqrt{|p|} \hat{d}_{|p|}, & p < 0, \\ \sqrt{p} \hat{d}_p^\dagger, & p > 0, \end{cases} \quad (11)$$

it is found that bosonic commutation relations

$$[\hat{d}_m, \hat{d}_n^\dagger] = \delta_{m,n}, \quad (12)$$

are satisfied after introducing the anomalous vacuum (cf. e.g., [23]).

The bosonized form of the backscattering operator is

$$\hat{V}_c = -\frac{1}{2} \sum_{m>0} m V_c(m) \{ \hat{d}_m^2 + \hat{d}_m^{\dagger 2} \} + \frac{1}{2} \sum_{m>0} \sqrt{2m} V_c(m) [\hat{d}_{2m} + \hat{d}_{2m}^\dagger]. \quad (13)$$

It is seen that the two-particle interaction due to backward scattering is of the same form as the forward scattering operator \hat{V}_b studied in [24], except for a sign change. Thus it amounts to the renormalization

$$\hat{V}_b \rightarrow \hat{V}_b - \hat{V}_c, \quad (14)$$

in complete analogy to the Luttinger case. However, the remaining one-particle operator produces non-trivial changes.

In order to diagonalize the total Hamiltonian

$$\tilde{H} = \hbar\omega_\ell \sum_{m>0} m \hat{d}_m^\dagger \hat{d}_m + \hat{V}, \quad (15)$$

with

$$\begin{aligned} \hat{V} &= \frac{1}{2} \sum_{m>0} m V_a(m) \{ \hat{d}_m^\dagger \hat{d}_m + \hat{d}_m \hat{d}_m^\dagger \} \\ &+ \frac{1}{2} \sum_{m>0} m [V_b(m) - V_c(m)] \{ \hat{d}_m^2 + \hat{d}_m^{\dagger 2} \} + \frac{1}{2} \sum_{m>0} V_c(m) \sqrt{2m} [\hat{d}_{2m} + \hat{d}_{2m}^\dagger], \end{aligned} \quad (16)$$

we perform two canonical transformations:

$$\hat{d}_m = \hat{S}_2^\dagger \{ \hat{S}_1^\dagger \hat{f}_m \hat{S}_1 \} \hat{S}_2. \quad (17)$$

The first one

$$\hat{S}_1 = \exp \left[\frac{1}{2} \sum_{m>0} \zeta_m (\hat{f}_m^2 - \hat{f}_m^{\dagger 2}) \right], \quad (18)$$

is a kind of squeezing transformation and was used in [24] to diagonalize the two-particle interactions. It gives

$$\{ \hat{S}_1^\dagger \hat{f}_m \hat{S}_1 \} = \hat{f}_m \cosh \zeta_m - \hat{f}_m^\dagger \sinh \zeta_m. \quad (19)$$

The second one

$$\hat{S}_2 = \exp \left[\sum_{m>0} \eta_m (\hat{f}_m^\dagger - \hat{f}_m) \right], \quad (20)$$

is a displacement in order to get rid of the terms linear in the \hat{d} and \hat{d}^\dagger operators. The total result is

$$\hat{d}_m = \hat{f}_m \cosh \zeta_m - \hat{f}_m^\dagger \sinh \zeta_m + \eta_m \exp(-\zeta_m). \quad (21)$$

We find two diagonalization conditions: The standard one

$$\tanh 2\zeta_m = \frac{V_b(m) - V_c(m)}{\hbar\omega_\ell + V_a(m)}, \quad (22)$$

and another one due to backscattering

$$\eta_m = \begin{cases} -V_c(m/2) \exp(-\zeta_m)/(2\sqrt{m} \epsilon_m), & m = 2n, \\ 0, & m = 2n - 1. \end{cases} \quad (23)$$

The final form of the Hamiltonian is

$$\tilde{H} = \tilde{H}_0 + \hat{V}_a + \hat{V}_b + \hat{V}_c = \sum_{m>0} m \epsilon_m \hat{f}_m^\dagger \hat{f}_m + \text{const.} \quad (24)$$

The renormalized oscillator frequencies are

$$\epsilon_m \equiv \sqrt{[\hbar\omega_\ell + V_a(m)]^2 - [V_b(m) - V_c(m)]^2}, \quad (25)$$

and

$$\exp(-\zeta_m) \equiv \sqrt{K_m} \quad (26)$$

defines the dimensionless coupling constants

$$K_m \equiv \sqrt{\frac{\hbar\omega_\ell + V_a(m) - V_b(m) + V_c(m)}{\hbar\omega_\ell + V_a(m) + V_b(m) - V_c(m)}}. \quad (27)$$

One-particle matrix elements

We apply the theory to the evaluation of the one-particle matrix elements $\langle \hat{c}_m^\dagger \hat{c}_n \rangle$. To this order, we follow the steps in [24] and introduce the bosonic field

$$\hat{\phi}^\dagger(v) = i \sum_{n=1}^{\infty} \frac{1}{\sqrt{n}} e^{-inv} \hat{d}_n^\dagger \neq \hat{\phi}(v), \quad (28)$$

which allows to express a particle number conserving bilinear product of auxiliary Fermi fields studied by Schönhammer and Meden [34]

$$\hat{\psi}_a(v) \equiv \sum_{l=-\infty}^{\infty} e^{ilv} \hat{c}_l = \hat{\psi}_a(v + 2\pi), \quad (29)$$

as

$$\hat{\psi}_a^\dagger(u) \hat{\psi}_a(v) = G_N(u - v) \exp \left\{ -i \left[\hat{\phi}^\dagger(u) - \hat{\phi}^\dagger(v) \right] \right\} \exp \left\{ -i \left[\hat{\phi}(u) - \hat{\phi}(v) \right] \right\}. \quad (30)$$

The quantity $G_N(u)$ in Eq. (30) is a distribution valued Fermi sum defined by

$$G_N(u) = \sum_{l=-\infty}^{N-1} e^{-il(u+i\epsilon)}. \quad (31)$$

In order to evaluate expectation values of exponentials containing $\hat{\phi}$ -operators, one must

- a) express the \hat{d} -operators in terms of the free \hat{f} and \hat{f}^\dagger -operators,
- b) apply the bosonic Wick theorem.

The Wick theorem refers to homogeneous linear combinations of \hat{f} and \hat{f}^\dagger -operators. Due to backscattering, the operator $\hat{\phi}$ contains a c-number part ϕ_c , which must be treated separately:

$$\phi_c(u) \equiv -iC(-u), \quad (32)$$

with

$$C(u) \equiv \sum_{m=1}^{\infty} \xi_{2m} \exp(-2imu). \quad (33)$$

The quantities ξ_{2m} are given by

$$\xi_{2m} \equiv \eta_{2m} \sqrt{\frac{K_{2m}}{2m}} = -V_c(m) \frac{K_{2m}}{4m \epsilon_{2m}}. \quad (34)$$

Following the steps in [24], the zero temperature expectation value of Eq. (30) becomes

$$\langle \hat{\psi}_a^\dagger(u) \hat{\psi}_a(v) \rangle = G_N(u-v) \exp[-W_1(u,v) - W_2(u,v)], \quad (35)$$

with W_1 given by

$$W_1(u,v) = \sum_{m>0} \frac{2}{m} [\gamma_m - \alpha_m \cos m(u+v)] \{1 - \cos m(u-v)\}. \quad (36)$$

The interaction parameters are

$$\alpha_m = \frac{1}{2} \sinh 2\zeta_m, \quad \gamma_m = \sinh^2 \zeta_m. \quad (37)$$

The contribution due to backscattering is:

$$W_2(u,v) = C(-u) - C(u) + C(v) - C(-v) = 4i \sum_{m=1}^{\infty} \xi_{2m} \sin m(u-v) \cos m(u+v). \quad (38)$$

In order to obtain the matrix elements, a number of calculational steps are done, starting with the coordinate transformation $(u+v)/2 = t$, $u-v = s$. Using $W_i(u,v) = \tilde{W}_i(s,t)$ and $\tilde{W}_i(s \pm 2\pi, t) = \tilde{W}_i(s, t \pm \pi) = \tilde{W}_i(s, t)$, ($i = 1, 2$) and further symmetries, one obtains

$$\langle \hat{c}_{n-p}^\dagger \hat{c}_{n+p} \rangle = \int_{-\pi}^{\pi} \frac{dt}{2\pi} \cos pt \int_{-\pi}^{\pi} \frac{ds}{2\pi} \exp[-\tilde{W}_1(s, t/2) - \tilde{W}_2(s, t/2)] \left\{ \frac{\exp[is(n-N+1)]}{1 - \exp(is - \epsilon)} \right\} \quad (39)$$

The distribution in curly brackets can be written as

$$\left\{ \frac{\exp[is(n-N+1)]}{1 - \exp(is - \epsilon)} \right\} = - \left\{ \frac{\sin(n-N+\frac{1}{2})s}{2 \sin(s/2)} \right\} + i \left[\frac{\cos(n-N+\frac{1}{2})s}{2 \sin(s/2)} \right] + \pi \delta_{2\pi}(s). \quad (40)$$

By defining

$$\tilde{W}_2(s, t/2) \equiv if(s, t), \quad (41)$$

the final result becomes

$$\begin{aligned} \langle \hat{c}_{n-p}^\dagger \hat{c}_{n+p} \rangle &= \frac{1}{2} \delta_{p,0} - \int_{-\pi}^{\pi} \frac{dt}{2\pi} \cos(pt) \\ &\times \int_{-\pi}^{\pi} \frac{ds}{2\pi} \left\{ \frac{\sin[(n - N + 1/2)s - f(s, t)]}{2 \sin(s/2)} \right\} \exp[-\tilde{W}_1(s, t/2)]. \end{aligned} \quad (42)$$

Besides modifications of the transformation parameters ζ_m in Eq. (22), the effect of backscattering appears in the argument of the sine via the function $f(s, t)$, which is explicitly given by

$$f(s, t) = 4 \sum_{m=1} \xi_{2m} \sin(ms) \cos(mt). \quad (43)$$

Backscattering thus destroys the specific form of particle-hole symmetry found in [24] for forward scattering.

IV. RESULTS

The functions $\tilde{W}_1(s, t)$ and $f(s, t)$ in the exact expression (42) for the matrix elements contain a bewildering number of interaction coefficients, which all depend on the index m . In order to proceed with the evaluation, we describe in the Appendix a model for the interaction coefficients, which allows to do all summations and express them by just two parameters: The main coupling constant K and a small number $r \ll 1$ specifying the exponential decay of all interaction coefficients. Following [25], we adopt $r = 1/\sqrt{N}$ so that only the coupling constant $K > 0$ remains. $K > 1$ corresponds to attractive interactions and $0 < K < 1$ to repulsion between the fermions. An analogous procedure is used in the theory of the Luttinger model [20, 21, 22, 23].

The result for the one-particle matrix elements becomes

$$\begin{aligned} \langle \hat{c}_{n-p}^\dagger \hat{c}_{n+p} \rangle &= \frac{\delta_{p,0}}{2} - \int_{-\pi}^{\pi} \frac{dt}{2\pi} \frac{\cos(pt)}{[1 + Z_\alpha - \cos(t)]^{\alpha_0}} \int_{-\pi}^{\pi} \frac{ds}{2\pi} \left\{ \frac{\sin[(n - N + 1/2)s - f(s, t)]}{2 \sin(s/2)} \right\} \\ &\times \left\{ \frac{Z_\gamma}{[1 + Z_\gamma - \cos(s)]} \right\}^{\gamma_0} \{ [1 + Z_\alpha - \cos(t - s)][1 + Z_\alpha - \cos(t + s)] \}^{\alpha_0/2}, \end{aligned} \quad (44)$$

with constants Z_γ and Z_α according to

$$Z_\gamma = \cosh(r_\gamma) - 1 \rightarrow r^2/2, \quad Z_\alpha = \cosh(r_\alpha/2) - 1 \rightarrow r^2/8. \quad (45)$$

The coupling dependent exponents in Eq. (44) are

$$\alpha_0 = \frac{1}{4K} (1 - K^2), \quad \gamma_0 = \frac{1}{4K} (1 - K)^2 \geq 0. \quad (46)$$

The sign of α_0 is negative when the backscattering is attractive.

In addition, we take advantage of the fact that backscattering is dominant in a harmonically confined gas of identical fermions: The function f is then determined by the backscattering contribution $C(u)$ in Eq. (A.90):

$$f(s, t) = 2\Im[C(t/2 - s/2) - C(t/2 + s/2)] = \frac{1}{4} (1 - K^2) \arctan \left[\frac{2q (\cos t - q \cos s) \sin s}{1 - q^2 - 2q (\cos t - q \cos s) \cos s} \right] \quad (47)$$

with

$$q = \exp(-r) \rightarrow 1 - r + r^2/2. \quad (48)$$

A. Analytic approximation

Equation (44) is still too complicated to allow an exact analytical treatment. We can, however, exploit the smallness of r to find an approximate analytic result: In a first approximation, the expression (47) for the function $f(s, t)$ reduces to

$$f(s, t) \rightarrow -\frac{1}{4} (1 - K^2) s. \quad (49)$$

Then we employ an improved version of the approximation described in Sec. V of [25, 35]. It is based on the observation that the factor

$$\left\{ \frac{Z_\gamma}{1 + Z_\gamma - \cos(s)} \right\}^{\gamma_0} \rightarrow \left[\frac{r^2}{r^2 + s^2} \right]^{\gamma_0}, \quad (50)$$

effectively restricts the s -integration in Eq. (44) to values $|s| < r$. This leads to

$$\langle \hat{c}_{n-p}^\dagger \hat{c}_{n+p} \rangle = \delta_{p,0} \left\{ \frac{1}{2} - r \int_0^{\pi/r} \frac{dx}{\pi} \left[\frac{\sin[(n - N + 1/2 - (K^2 + 1)/4) r x]}{2 \sin(r x/2)} \right] \left[\frac{1}{1 + x^2} \right]^{\gamma_0} \right\}. \quad (51)$$

With the further reasonable approximations $2 \sin(rx/2) \rightarrow rx$ and $\pi/r \rightarrow \infty$, a solvable integral in terms of generalized hypergeometric functions is obtained. For $\gamma_0 \neq 1/2$, we find

$$\begin{aligned} \langle \hat{c}_{n-p}^\dagger \hat{c}_{n+p} \rangle = \delta_{p,0} & \left\{ \frac{1}{2} - \frac{a_n}{2\sqrt{\pi}} \left[\frac{\Gamma(\gamma_0 - 1/2)}{\Gamma(\gamma_0)} {}_1F_2(1/2; 3/2 - \gamma_0, 3/2; a_n^2/4) \right. \right. \\ & \left. \left. + \left(\frac{a_n^2}{4} \right)^{\gamma_0 - 1/2} \frac{\Gamma(1/2 - \gamma_0)}{2\Gamma(\gamma_0 + 1)} {}_1F_2(\gamma_0; \gamma_0 + 1/2, \gamma_0 + 1; a_n^2/4) \right] \right\}. \end{aligned} \quad (52)$$

The quantity a_n is defined by

$$a_n \equiv [n - N + 1 - (K^2 + 1)/4] r. \quad (53)$$

It is small near the Fermi edge but becomes large away from it.

For $\gamma_0 = 1/2$, we find in terms of a Bessel function

$$\langle \hat{c}_{n-p}^\dagger \hat{c}_{n+p} \rangle = \delta_{p,0} \left[\frac{1}{2} - \frac{1}{\pi} \int_0^{a_n} dx K_0(x) \right]. \quad (54)$$

It is seen that in this approximation the matrix elements remain diagonal. The sign of the interaction enters only via K in Eq. (53). The non-interacting limit $K \rightarrow 1$ is correctly reproduced by Eq. (52):

$$\langle \hat{c}_n^\dagger \hat{c}_n \rangle = \Theta(N - n - 1/2). \quad (55)$$

The approximation works reasonably well in the full range of n -values with the largest (but still small) error near the Fermi edge as shown in Fig. 1 for an attractive interaction.

It is noted that the diagonal matrix elements

$$P_n \equiv \langle \hat{c}_n^\dagger \hat{c}_n \rangle \quad (56)$$

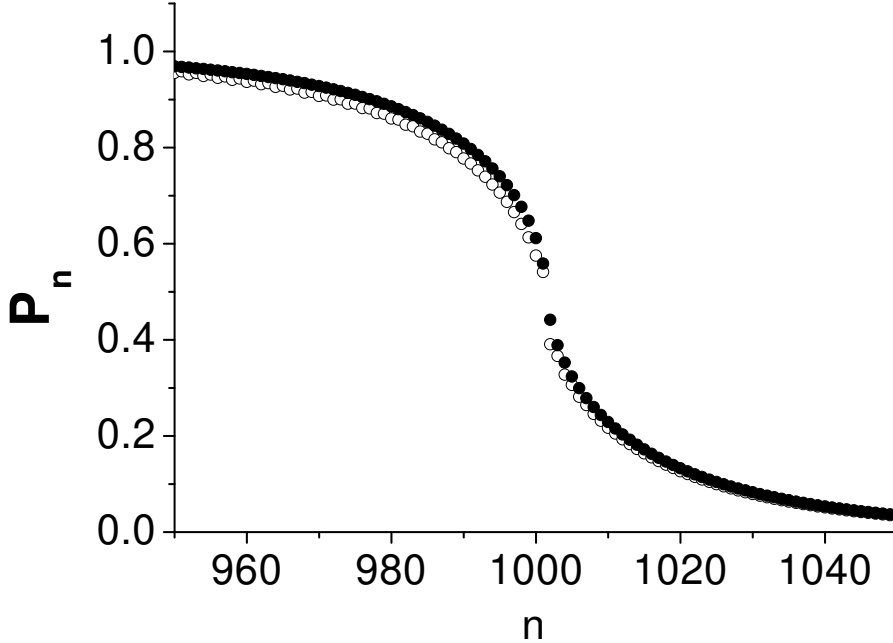


FIG. 1: Occupation probabilities of oscillator states ψ_n near the Fermi edge $n = N - 1$ at zero temperature for $N=1000$ trapped fermions. Open circles are from the complete theory according to Eq. (44) while full circles are calculated using the analytic approximation (52). An attractive interaction with coupling strength $K = 3$ is assumed.

have the meaning of occupation probabilities of oscillator states ψ_n .

Exact numerical evaluation of Eq. (44) shows that non-diagonal one-particle matrix elements are generated by the interactions. They are reasonably small for attractive interactions or moderate repulsive coupling, when $K < 1$ is still of order unity. They become, however, relevant for strong repulsion ($K \ll 1$). The analytic approximation (52) fails in this limit.

B. Particle and momentum densities

The particle density $n(z)$ is related to the one-particle matrix elements by

$$n(z) = \sum_{n=0}^{\infty} \sum_{p=-n}^n \psi_{n-p}(z) \psi_{n+p}(z) \langle \hat{c}_{n-p}^\dagger \hat{c}_{n+p} \rangle. \quad (57)$$

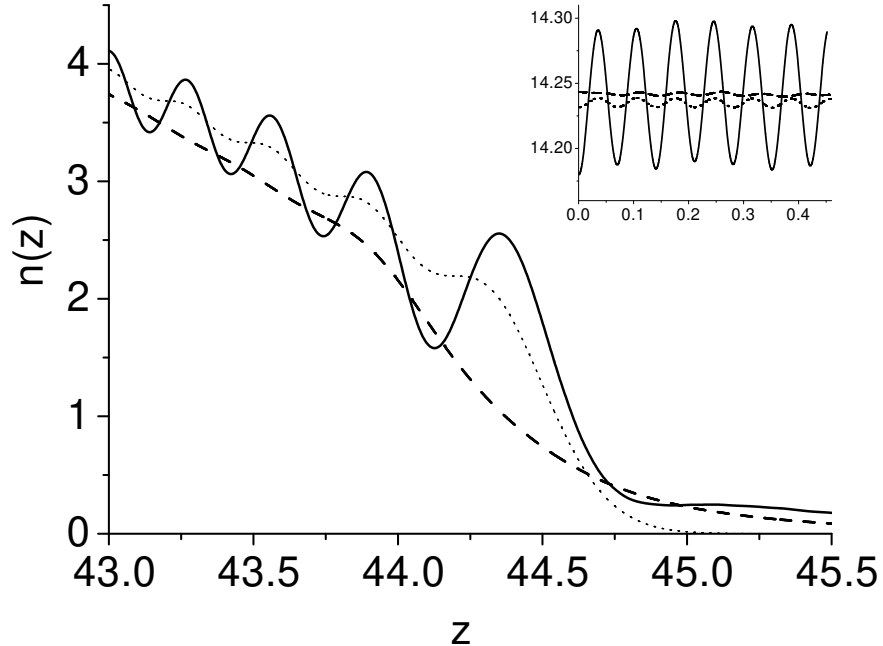


FIG. 2: Dimensionless particle density $n(z)$ in units of the inverse of the oscillator length l versus dimensionless distance z near the classical boundary at $L_F = \sqrt{2N-1}$ of the one-dimensional harmonic trap for $N = 1000$ interacting spinless fermions at zero temperature. Dotted curve shows unperturbed Friedel oscillations. Strongly oscillating curve refers to a repulsive interaction with $K = 1/3$ while the dashed curve is for an attractive interaction with $K = 3$. The inset displays the density near the center of the trap, where Friedel oscillation have the usual period $\pi/k_F = \pi/\sqrt{2N-1}$.

For large N and moderate coupling (K is of order unity), the particle density well inside the trap is dominated by the large number of nearly filled states inside the Fermi sea. However, the states above the Fermi level $N_F = N - 1$, seen in Fig. 1, make significant contributions to $n(z)$ by modifying the Friedel oscillations [36]: This is demonstrated in Fig. 2 using the full expression (44).

It is seen that Friedel oscillations are enhanced in the repulsive case while an attractive interaction suppresses them. Near the classical boundary $|z| \approx L_F = \sqrt{2N-1}/\alpha$, the oscillation period is larger than the standard value π/k_F well inside the trap and obeys the relations found in [37] for the non-interacting case. Furthermore, it is seen that the perturbed density extends considerably into the classically forbidden region. The effect

becomes stronger with increasing coupling strength ($K \gg 1$ or $\ll 1$).

The momentum density distribution is given by

$$p(k) = \frac{1}{\alpha^2} \sum_{n=0}^{\infty} \sum_{p=-n}^n (-1)^p \psi_{n-p}(k/\alpha^2) \psi_{n+p}(k/\alpha^2) \langle \hat{c}_{n-p}^\dagger \hat{c}_{n+p} \rangle. \quad (58)$$

It is seen that $p(k)$ is identical in shape to the density distribution $n(z)$ provided the diagonal approximation for the one-particle matrix elements is reasonable. This is the case for moderate attractive coupling.

We know [24] that the Friedel oscillations in $n(z)$ and $p(k)$ behave oppositely: Attractive interactions increase them in the momentum density and decrease them in the particle density and vice versa for repulsion. A corresponding effect is seen in the Wigner function discussed below.

C. Wigner function

In terms of the local creation and annihilation operators $\hat{\psi}^\dagger(z)$ and $\hat{\psi}(z)$, the static Wigner function of the many-fermion system is given (cf. [38]) by

$$W(z, k) = \int_{-\infty}^{\infty} d\zeta e^{-ik\zeta} \langle \hat{\psi}^\dagger(z - \zeta/2) \hat{\psi}(z + \zeta/2) \rangle. \quad (59)$$

The Wigner function of the one-dimensional Fermi gas with two components and forward scattering between the two components was studied in [39].

Transforming to the oscillator representation gives

$$W(z, k) = \sum_{m,n=0}^{\infty} \langle \hat{c}_m^\dagger \hat{c}_n \rangle f_{mn}(z, k), \quad (60)$$

with expansion coefficients f_{mn} according to

$$f_{mn}(z, k) = \int_{-\infty}^{\infty} d\zeta e^{-ik\zeta} \psi_m(z - \zeta/2) \psi_n(z + \zeta/2) = f_{nm}(z, -k). \quad (61)$$

These are explicitly given in terms of generalized Laguerre polynomials ($n \geq m$, cf. e.g., [40]) by:

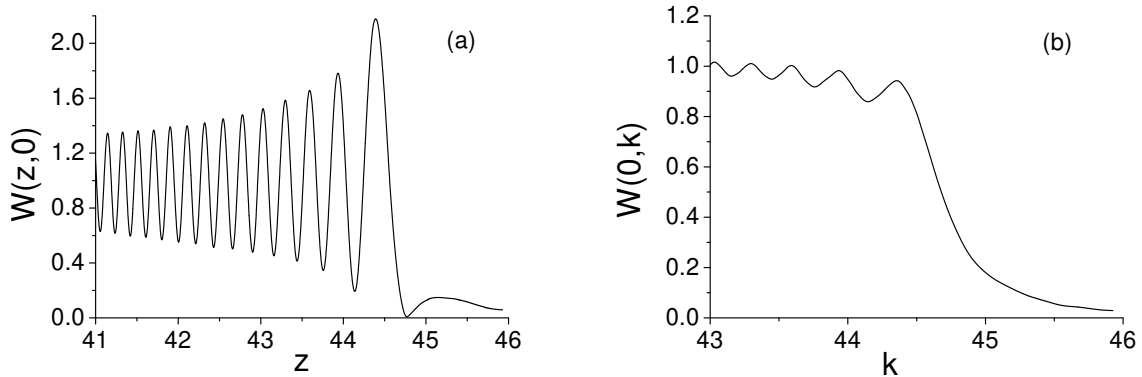


FIG. 3: Friedel oscillations in phase space: Wigner function for $N = 1000$ interacting spinless fermions at zero temperature in the one-dimensional harmonic trap. In (a), the cross section $W(z, k = 0)$ is plotted versus dimensionless distance z displaying the region around the classical turning point $\sqrt{2N - 1}$. In (b), the corresponding function $W(z = 0, k)$ is shown versus dimensionless momentum k . Note the increase of the oscillation amplitude near the classical boundary. The plot refers to a repulsive interaction with $K = 1/3$. Repulsive interactions enhance Friedel oscillations in the spatial direction and suppress them in the momentum direction.

$$f_{mn}(z, k) = 2(-1)^m (2^{n-m} m! / n!)^{1/2} (\alpha z - ik/\alpha)^{n-m} \exp(-\alpha^2 z^2 - k^2/\alpha^2) L_m^{(n-m)}(2\alpha^2 z^2 + 2k^2/\alpha^2) \quad (62)$$

It is noted that the one-particle matrix elements can be completely reconstructed from the Wigner function:

$$\langle \hat{c}_m^\dagger \hat{c}_n \rangle = \frac{1}{2\pi} \int_{-\infty}^{\infty} dz dk f_{nm}(z, k) W(z, k). \quad (63)$$

The Wigner function is thus equivalent to the full set of one-particle matrix elements.

We show an example of the Wigner function in Figs. 3(a) and 3(b) for a repulsive interaction.

The amplitudes of the Friedel oscillations increase near the classical turning point. This was discussed for the non-interacting case [37].

Neglecting non-diagonal matrix elements in Eq. (60) would give $W(z, k = 0) = W(z = 0, k \rightarrow \alpha^2 z)$. The significant differences between Fig. 3(a) and Fig. 3(b) thus stem from the non-diagonal matrix elements, which are particularly relevant for repulsive interactions.

The static pair correlation function with respect to the center of the trap

$$C(z, z' = 0) \equiv \langle \hat{\psi}^\dagger(z) \hat{\psi}(z' = 0) \rangle = \frac{1}{2\pi} \int_{-\infty}^{\infty} dk e^{-ikz} W(z/2, k), \quad (64)$$

as well as any other one-particle property of the many-particle system are also contained in the Wigner function.

The central pair correlation function (64) is displayed in Fig. 4. It is noted that the wave length of the intrinsic periodicity in the center of the trap is twice that of the Friedel oscillations, i.e., $\lambda = 2\pi/k_F$. In fact, the central pair correlation function for non-interacting fermions is given by

$$C_0(z, z' = 0) = \frac{\alpha}{\sqrt{\pi}} e^{-\alpha^2 z^2/2} \left[\sum_{n=0}^M (-1)^n \frac{H_{2n}(\alpha z)}{4^n n!} \right] \rightarrow \frac{\sin(k_F z)}{\pi z}, \quad (65)$$

provided $N = 2M$ is large and z is restricted to the center of the trap ($|z| \ll L_F$). We expect that interactions modify Eq. (65) according to

$$C(l \ll z \ll L_F, z' = 0) \propto \alpha \frac{\sin(k_F z)}{(\alpha z)^{\alpha_C}}, \quad (66)$$

i.e., the anomalous dimension of the correlation function is $\alpha_C = 1 + 2\gamma_0 = (K + 1/K)/2$, as in a Luttinger liquid. This is confirmed numerically by displaying the corresponding envelope in Fig. 4.

The correlation function C of the interacting system thus decays faster than C_0 and this effect is invariant under $K \rightarrow 1/K$.

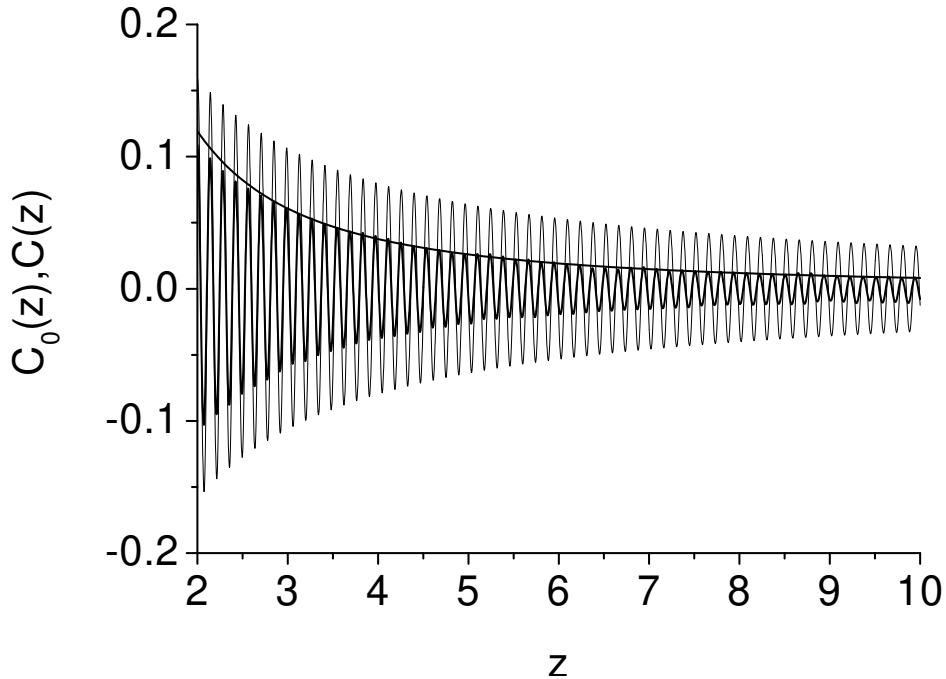


FIG. 4: Dimensionless correlation function $C(z, z' = 0)$ in units of the inverse of the oscillator length l versus dimensionless distance z from the center of the trap for $N = 1000$ interacting spinless fermions at zero temperature. Thin curve shows non-interacting case while the thick curve is for an attractive interaction with $K = 3$. Oscillations have twice the period of Friedel oscillations. Envelope to the full curve displays power law decay with anomalous dimension $(K + 1/K)/2$.

V. SUMMARY

The fact that backscattering dominates the interaction between identical one-dimensional fermions confined to a harmonic trap makes it necessary to include backscattering into the bosonization method. This can be done exactly by supplementing the squeezing transformation (18) with the displacement transformation (20). This changes (in fact complicates) the result (42) for the one-particle matrix elements by altering the argument in the sine-function. This modification destroys the symmetry

$$\langle \hat{c}_{2N-1-n-p}^\dagger \hat{c}_{2N-1-n+p} \rangle = \delta_{p,0} - \langle \hat{c}_{n-p}^\dagger \hat{c}_{n+p} \rangle. \quad (67)$$

In order to evaluate the new result, we introduce in analogy to the Luttinger model

a simplified form for the interaction coefficients which uses only one coupling constant K . $K = 1$ corresponds to the non-interacting case studied in [37, 41, 42, 43], $K > 1$ corresponds to attraction. For modest values of $K > 1$, an analytical approximation for the matrix elements, which then remain nearly diagonal, is derived. The Fermi edge at zero temperature is already significantly smoothed out by the interactions, an effect which becomes more pronounced for stronger coupling.

We then study particle and momentum densities for various coupling strengths. Friedel oscillations in phase space are characteristic for these quantities, which extend progressively into the classically forbidden region when the coupling strength is increased. The results confirm an earlier finding that attractive interactions decrease the amplitude of the Friedel oscillations in real space while repulsion enhances it. The Friedel oscillations in momentum space behave oppositely.

Finally, the central pair correlation function is calculated. The basic period of the pair correlation function in the center of the trap is $2\pi/k_F$ in contrast to π/k_F of the Friedel oscillations. Interactions do not affect these basic periodicities: Even the increase of the Friedel period in the particle density near the classical boundaries is correctly given by the non-interacting theory. Interactions, however, modify the power law decay of the correlation function inside the trap. Our numerical results are consistent with the value

$$\alpha_C = \frac{K + 1/K}{2} \tag{68}$$

for the anomalous dimension α_C of the correlation well inside the trap, in accordance with the predictions for a Luttinger liquid.

Acknowledgments

We gratefully acknowledge helpful discussions with G. Alber, F. Gleisberg, T. Pfau, and W. P. Schleich and financial help by Deutsche Forschungsgemeinschaft.

A MODEL FOR THE INTERACTION COEFFICIENTS

The result (42) for the one-particle matrix elements contains three sets of interaction coefficients: $\{\alpha_m\}$, $\{\gamma_m\}$, and $\{V_c(m)\}$. The first two sets depend on the basic interaction

coefficients $V_a(m)$, $V_b(m)$, and $V_c(m)$ via the parameter ζ_m according to Eq. (22). The third set $V_c(m)$, related to backscattering, appears directly in W_2 . In order to get explicit results for the matrix elements, one must be able to perform the summations in \tilde{W}_1 and \tilde{W}_2 . This requires models for the m -dependence of the above interaction coefficients.

Defining $\tilde{V} \equiv V/\hbar\omega_\ell$, an explicit form for α_m is

$$\alpha_m = \frac{\tilde{V}_b(m) - \tilde{V}_c(m)}{2\sqrt{(1 + \tilde{V}_a(m))^2 - (\tilde{V}_b(m) - \tilde{V}_c(m))^2}} \equiv \frac{1 - K_m^2}{4K_m}. \quad (\text{A.69})$$

Similarly, the central coupling constants K_m determine γ_m and the renormalized oscillator energies ϵ_m according to

$$\gamma_m = \frac{(1 - K_m)^2}{4K_m}, \quad \epsilon_m = \hbar\omega_\ell \frac{2K_m}{K_m^2 + 1} [1 + \tilde{V}_a(m)]. \quad (\text{A.70})$$

Following the procedure in the Luttinger model, we adopt exponential decays, thus we make the ansatz:

$$\alpha_m = \alpha_0 \exp(-r_\alpha m/2), \quad (\text{A.71})$$

and

$$\gamma_m = \gamma_0 \exp(-r_\gamma m). \quad (\text{A.72})$$

Since the signs of $\tilde{V}_b(m)$ and $\tilde{V}_c(m)$ do not depend on m , α_m is related to γ_m by

$$\alpha_m = \text{sgn}(\tilde{V}_b - \tilde{V}_c) \sqrt{\gamma_m(1 + \gamma_m)}, \quad (\text{A.73})$$

and one finds

$$\alpha_m = \text{sgn}(\tilde{V}_b - \tilde{V}_c) \exp(-r_\gamma m/2) \sqrt{\gamma_0(1 + \gamma_0 \exp(-r_\gamma m))}. \quad (\text{A.74})$$

Assuming that r_γ is very small, $0 < r_\gamma \ll 1$, and that the relevant values of m obey $m < 1/r_\gamma$, Eq. (A.74) leads to

$$\alpha_m = \exp(-r_\gamma m/2) \alpha_0, \quad (\text{A.75})$$

with

$$\alpha_0 = \text{sgn}(\tilde{V}_b - \tilde{V}_c) \sqrt{\gamma_0(1 + \gamma_0)}. \quad (\text{A.76})$$

Thus, we can set

$$r_\alpha = r_\gamma \equiv r. \quad (\text{A.77})$$

Another set of coupling parameters involves directly the backscattering coefficients $\tilde{V}_c(m)$ via ξ_{2m} in \tilde{W}_2 . Using Eqs. (25) and (27), Eq. (34) becomes

$$\xi_{2m} = -\frac{\tilde{V}_c(m)}{4m[1 + \tilde{V}_a(2m) + \tilde{V}_b(2m) - \tilde{V}_c(2m)]}. \quad (\text{A.78})$$

The explicit appearance of $\tilde{V}_c(m)$ makes it necessary to introduce a second coupling constant K_c besides K . We take advantage of the slow decay of interaction coefficients with m and write

$$\xi_{2m} = -\frac{1}{4m} \tilde{V}_{eff} \exp(-r_c m), \quad (\text{A.79})$$

with another decay constant $r_c \ll 1$ and with

$$\tilde{V}_{eff} \approx \frac{\tilde{V}_c(1)}{1 + \tilde{V}_a(1) + \tilde{V}_b(1) - \tilde{V}_c(1)} \equiv \left\{ \frac{\tilde{V}_c(1)}{2[1 + \tilde{V}_a(1)]} \right\} (1 + K^2). \quad (\text{A.80})$$

This gives a useful result for the backscattering function (33)

$$C(u) = -\frac{\tilde{V}_{eff}}{4} \sum_{m=1}^{\infty} \frac{1}{m} \exp[(-m(2iu + r_c))] = \frac{\tilde{V}_{eff}}{4} \ln[1 - \exp(-r_c - 2iu)]. \quad (\text{A.81})$$

The quantity in curly brackets in (A.80) will be taken as the second coupling constant

$$K_c = \frac{\tilde{V}_c(1)}{2[1 + \tilde{V}_a(1)]}. \quad (\text{A.82})$$

For large N , the forward interaction coefficients become equal, $\tilde{V}_a(1) \rightarrow \tilde{V}_b(1) \equiv \tilde{V}$ [24]. One then has a mapping between the initial coupling coefficients \tilde{V} and $\tilde{V}_c(1) \equiv \tilde{V}_c$ and the new coupling constants according to

$$\tilde{V} = \frac{1 - K^2 + 2K_c(1 + K^2)}{2[K^2 - K_c(1 + K^2)]}, \quad (\text{A.83})$$

and

$$\tilde{V}_c = \frac{K_c(1 + K^2)}{2[K^2 - K_c(1 + K^2)]}. \quad (\text{A.84})$$

It is noted that consistency requires $\tilde{V} \geq -1$, $\tilde{V}_c \geq -1$, $\tilde{V}_c \leq 1 + 2\tilde{V}$, $-\infty < K_c < K^2/(1 + K^2)$, and $K \geq 0$.

This general frame is still rather complicated for applications. We can get rid of K_c , however, by utilizing the following feature: Studies of the interaction coefficients showed [33] that any effective one-dimensional local pair interaction $V_{1Def}(z)$ between identical fermions in a harmonic trap suppresses forward scattering in the sense of $|\tilde{V}| \ll |\tilde{V}_c|$, unless the interaction is of long range. The quantitative condition is the existence of a Fourier transform $\tilde{V}_{1Def}(k)$ which is regular at $k = 0$. It is satisfied, e.g., for the dipole-dipole interaction in one dimension.

In the following, we set $\tilde{V} = 0$ and consider only \tilde{V}_c . This will allow us to relate ξ_{2m} to α_m : The simplified version of (A.69) is

$$\alpha_m = -\frac{\tilde{V}_c(m)}{2\sqrt{1 - \tilde{V}_c^2(m)}}. \quad (\text{A.85})$$

Comparing $\alpha(m)$ in Eq. (A.85) with Eq. (A.78), leads to

$$\alpha_m = -\tilde{V}_{eff} \exp(-r_c m) \left\{ \frac{1 - \tilde{V}_c(2m)}{2\sqrt{1 - \tilde{V}_c^2(m)}} \right\}. \quad (\text{A.86})$$

Suppressing the weak m -dependence in the curly brackets, i.e.,

$$\tilde{V}_c(m) \rightarrow \tilde{V}_c, \quad (\text{A.87})$$

allows the identifications

$$r_c = \frac{r_\alpha}{2} = \frac{r}{2}. \quad (\text{A.88})$$

Furthermore, using

$$\alpha_0 \equiv -\frac{\tilde{V}_c}{2\sqrt{1 - \tilde{V}_c^2}}, \quad (\text{A.89})$$

gives

$$\tilde{V}_{ceff} = -2 \sqrt{\frac{1 + \tilde{V}_c}{1 - \tilde{V}_c}} \alpha_0. \quad (\text{A.90})$$

The main coupling constant

$$K = \sqrt{\frac{1 + \tilde{V}_c}{1 - \tilde{V}_c}} \quad (\text{A.91})$$

determines all relevant couplings and the renormalized energy according to

$$\tilde{V}_c = \frac{K^2 - 1}{K^2 + 1}, \quad \alpha_0 = -\frac{K^2 - 1}{4K}, \quad \gamma_0 = \frac{(K - 1)^2}{4K}, \quad (\text{A.92})$$

$$\tilde{V}_{ceff} = \frac{1}{2} (K^2 - 1), \quad \epsilon = \hbar\omega_\ell \frac{2K}{K^2 + 1}.$$

Only the two parameters K and $r = r_\alpha = r_\gamma = 2r_c$ remain. K is determined by the physical backscattering strength $V_c(1) \equiv \tilde{V}_c$ according to Eq. (A.91). In [25], it was argued that $r = 1/\sqrt{N}$ is a reasonable choice for the decay constant. Finally, it is noted that interactions always decrease the renormalized excitation energy ϵ below the non-interacting value $\hbar\omega_\ell$.

-
- [1] M. H. Anderson *et al.*, *Science* **269**, 198 (1995); K. B. Davis *et al.*, *Phys. Rev. Lett.* **75**, 3969 (1995); C. C. Bradley *et al.*, *ibid.* **75**, 1687 (1995).
- [2] F. Brosens, J. T. Devreese, and L. F. Lemmens, *Phys. Rev. E* **57**, 3871 (1998).
- [3] G. M. Bruun and K. Burnett, *Phys. Rev. A* **58**, 2427 (1998).
- [4] M. A. Zaluska-Kotur, M. Gajda, A. Orłowski, and J. Mostowski, *Phys. Rev. A* **61**, 033613 (2000).
- [5] M. Houbiers *et al.*, *Phys. Rev. A* **56**, 4864 (1997).
- [6] M. A. Baranov and D. S. Petrov, *Phys. Rev. A* **58**, R801 (1998).
- [7] M. Houbiers and H. T. C. Stoof, *Phys. Rev. A* **59**, 1556 (1999).
- [8] R. Combescot, *Phys. Rev. Lett.* **83**, 3766 (1999).
- [9] B. DeMarco and D. S. Jin, *Science* **285**, 1703 (1999).
- [10] K. M. O’Hara *et al.*, *Phys. Rev. Lett.* **85**, 2092 (2000).
- [11] F. Schreck *et al.*, *Phys. Rev. A* **64**, 011402(R) (2001).
- [12] A. G. Truscott *et al.*, *Science* **291**, 2570 (2001).
- [13] F. Schreck *et al.*, *Phys. Rev. Lett.* **87**, 080403 (2001).
- [14] V. Vuletic *et al.*, *Phys. Rev. Lett.* **80**, 1634 (1998).
- [15] J. Fortagh, A. Grossmann, C. Zimmermann, and T. W. Hänsch, *Phys. Rev. Lett.* **81**, 5310 (1998).
- [16] J. Denschlag, D. Cassettari, and J. Schmiedmayer, *Phys. Rev. Lett.* **82**, 2014 (1999).
- [17] J. Reichel, W. Hänsel, and T. W. Hänsch, *Phys. Rev. Lett.* **83**, 3398 (1999).
- [18] H. Ott *et al.*, *Phys. Rev. Lett.* **87**, 230401 (2001).
- [19] H. L. Bethlem *et al.*, *Nature (London)* **406**, 491 (2000).
- [20] V. J. Emery, *Theory of the One-Dimensional Electron Gas*, in *Highly Conducting One-Dimensional Solids*, edited by J. T. Devreese, R. P. Evard, and V. E. van Doren (Plenum, New York, 1979), p247.
- [21] F. D. M. Haldane, *J. Phys. C: Solid State Phys.* **14**, 2585 (1981).
- [22] J. Voit, *Rep. Prog. Phys.* **58**, 977 (1995).
- [23] H. J. Schulz, *Fermi Liquids and Non-Fermi Liquids*, in *Mesoscopic Quantum Physics*, edited by E. Akkermans, G. Montambaux, J.-L. Pichard, and J. Zinn-Justin (Elsevier, Amsterdam,

- 1995), p533.
- [24] W. Wonneberger, Phys. Rev. A **63**, 063607 (2001).
 - [25] Gao Xianlong and W. Wonneberger, Phys. Rev. A **65**, 033610 (2002).
 - [26] J. L. Cardy, J. Phys. A **17**, L385 (1984).
 - [27] S. Eggert and I. Affleck, Phys. Rev. B **46**, 10866 (1992).
 - [28] M. Fabrizio and A. O. Gogolin, Phys. Rev. B **51**, 17827 (1995).
 - [29] R. Egger and H. Grabert, Phys. Rev. Lett. **75**, 3505 (1995).
 - [30] Y. Wang, J. Voit, and Fu-Cho Pu, Phys. Rev. B **54**, 8491 (1996).
 - [31] A. E. Mattsson, S. Eggert, and H. Johannesson, Phys. Rev. B **56**, 15615 (1997).
 - [32] J. Voit, Yupeng Wang, and M. Grioni, Phys. Rev. B **61**, 7930 (2000).
 - [33] F. Gleisberg and W. Wonneberger, unpublished.
 - [34] K. Schönhammer and V. Meden, Am. J. Phys. **64**, 1168 (1996).
 - [35] Formula (42) in Sec. V of [25] contains a factor r_γ in front of L_F which is wrong. Furthermore, the generalized hypergeometric function ${}_3F_2$ reduces exactly to the more familiar hypergeometric function ${}_2F_1(\bar{\gamma}_0, 1/2; 3/2; -\pi^2/r_\gamma^2)$. The conclusions remain unchanged.
 - [36] J. Friedel, Nuovo Cimento Suppl. **7**, 287 (1958).
 - [37] F. Gleisberg, W. Wonneberger, U. Schlöder, and C. Zimmermann, Phys. Rev. A **62**, 063602 (2000).
 - [38] M. Hillery, R. F. O’Connell, M. O. Scully, and E. P. Wigner, Phys. Rep. **106** (1984) 121.
 - [39] F. Gleisberg, W. P. Schleich, and W. Wonneberger, J. Phys. B: At. Mol. Opt. Phys. **34**, 4645 (2001).
 - [40] W. P. Schleich, *Quantum Optics in Phase Space*, (Berlin, Wiley-VCH, 2001).
 - [41] P. Vignolo, A. Minguzzi, and M. P. Tosi, Phys. Rev. Lett. **85**, 2850 (2000).
 - [42] A. Minguzzi, P. Vignolo, and M. P. Tosi, Phys. Rev. A **63**, 063604 (2001).
 - [43] P. Vignolo, A. Minguzzi, and M. P. Tosi, Phys. Rev. A **64**, 023421 (2001).

Figure Captions

Fig. 1: Occupation probabilities of oscillator states ψ_n near the Fermi edge $n = N - 1$ at zero temperature for $N=1000$ trapped fermions. Open circles are from the complete theory according to Eq. (44) while full circles are calculated using the analytic approximation (52). An attractive interaction with coupling strength $K = 3$ is assumed.

Fig. 2: Dimensionless particle density $n(z)$ in units of the inverse of the oscillator length l versus dimensionless distance z near the classical boundary at $L_F = \sqrt{2N - 1}$ of the one-dimensional harmonic trap for $N = 1000$ interacting spinless fermions at zero temperature. Dotted curve shows unperturbed Friedel oscillations. Strongly oscillating curve refers to a repulsive interaction with $K = 1/3$ while the dashed curve is for an attractive interaction with $K = 3$. The inset displays the density near the center of the trap, where Friedel oscillations have the usual period $\pi/k_F = \pi/\sqrt{2N - 1}$.

Fig. 3: Friedel oscillations in phase space: Wigner function for $N = 1000$ interacting spinless fermions at zero temperature in the one-dimensional harmonic trap. In (a), the cross section $W(z, k = 0)$ is plotted versus dimensionless distance z displaying the region around the classical turning point $\sqrt{2N - 1}$. In (b), the corresponding function $W(z = 0, k)$ is shown versus dimensionless momentum k . Note the increase of the oscillation amplitude near the classical boundary. The plot refers to a repulsive interaction with $K = 1/3$. Repulsive interactions enhance Friedel oscillations in the spatial direction and suppress them in the momentum direction.

Fig. 4: Dimensionless correlation function $C(z, z' = 0)$ in units of the inverse of the oscillator length l versus dimensionless distance z from the center of the trap for $N = 1000$ interacting spinless fermions at zero temperature. Thin curve shows non-interacting case while the thick curve is for an attractive interaction with $K = 3$. Oscillations have twice the period of Friedel oscillations. Envelope to the full curve displays power law decay with anomalous dimension $(K + 1/K)/2$.